

In Vitro Phosphorylation of the Focal Adhesion Targeting Domain of Focal Adhesion Kinase by Src Kinase

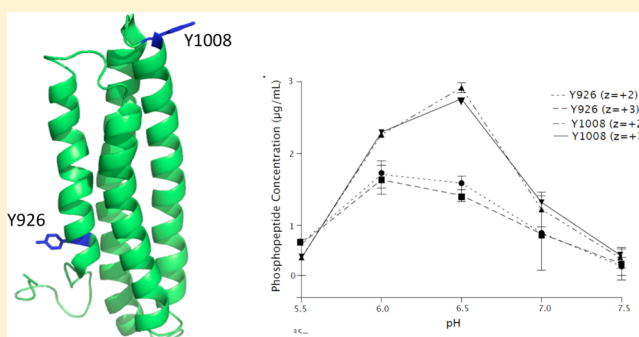
Jennifer Cable,[†] Kirk Prutzman,[†] Harsha P. Gunawardena,^{†,§} Michael D. Schaller,^{||} Xian Chen,^{†,§} and Sharon L. Campbell^{*,†,‡}

[†]Department of Biochemistry and Biophysics, [‡]Lineberger Comprehensive Cancer Center, and [§]Program in Molecular Biology and Biotechnology, University of North Carolina at Chapel Hill, Chapel Hill, North Carolina 27599, United States

^{||}Department of Biochemistry, West Virginia University, Morgantown, West Virginia 26506, United States

S Supporting Information

ABSTRACT: Focal adhesion kinase (FAK), a key regulator of cell adhesion and migration, is overexpressed in many types of cancer. The C-terminal focal adhesion targeting (FAT) domain of FAK is necessary for proper localization of FAK to focal adhesions and subsequent activation. Phosphorylation of Y926 in the FAT domain by the tyrosine kinase Src has been shown to promote metastasis and invasion in vivo by linking the FAT domain to the MAPK pathway via its interaction with growth factor receptor-bound protein 2. Several groups have reported that inherent conformational dynamics in the FAT domain likely regulate phosphorylation of Y926; however, what regulates these dynamics is unknown. In this paper, we demonstrate that there are two sites of in vitro Src-mediated phosphorylation in the FAT domain: Y926, which has been shown to affect FAK function in vivo, and Y1008, which has no known biological role. The phosphorylation of these two tyrosine residues is pH-dependent, but this does not reflect the pH dependence of Src kinase activity. Circular dichroism and nuclear magnetic resonance data indicate that the stability and conformational dynamics of the FAT domain are sensitive to changes in pH over a physiological pH range. In particular, regions of the FAT domain previously shown to regulate phosphorylation of Y926 as well as regions near Y1008 show pH-dependent dynamics on the microsecond to millisecond time scale.



Focal adhesion kinase (FAK) is a nonreceptor tyrosine kinase. Upon activation of integrins, FAK is recruited to newly forming focal adhesions where it functions as both a signaling protein and a scaffolding protein. It has been linked to the MAPK¹ and Rho and Ras GTPase^{2–4} pathways and plays a role in cell adhesion,^{5,6} migration,⁵ cell cycle progression,⁷ and cell survival.^{8–12} FAK consists of an N-terminal FERM (protein 4.1, ezrin, radixin, moesin) domain, a central kinase domain, and a C-terminal focal adhesion targeting (FAT) domain, which is responsible for the localization of FAK to focal adhesions at least partially through its interaction with the protein paxillin.¹³ The FAK kinase domain is activated by autophosphorylation at Y397, creating a Src homology (SH) 2 binding site that is recognized by Src kinase, among other proteins. Upon binding to Y397, Src phosphorylates several tyrosine residues in FAK, including Y926 in the FAT domain.^{10,14} Phosphorylation of Y926 creates a docking site for the SH2 domain of growth factor receptor-bound protein 2 (Grb2).^{10,14,15} The interaction between Grb2 and pY926 in the FAT domain has been shown to activate the MAPK pathway, resulting in an increased level of angiogenesis via upregulation of vascular endothelial growth factor (VEGF),^{16,17} and to promote microtubule-induced focal adhesion disassembly by

linking FAK to dynamin.¹⁸ Moreover, melanoma cells expressing a nonphosphorylatable Y926F mutant of FAK showed decreased levels of adhesion, migration, and invasion in vitro, which correlated with a decreased level of metastasis in vivo. These results reveal the importance of phosphorylation of Y926 in cell migration and adhesion and subsequently in cancer progression.¹⁶

There are several structures of the FAT domain, including a solution structure at pH 6.0¹⁹ and two crystal structures at pH 7.0,^{20,21} in which the FAT domain adopts an antiparallel four-helix bundle conformation. In addition, a crystal structure at pH 6.5 in which the FAT domain exists as a domain-swapped dimer in which helix 1 partitions away from the bundle and packs against the other three helices of a second FAT molecule has been determined.²¹ The ability of helix 1 to adopt both intra- and interdomain helix bundle conformations suggests that helix 1 possesses conformational mobility, and indeed, several lines of evidence, including nuclear magnetic resonance (NMR) and molecular dynamics simulations, have indicated

Received: January 26, 2012

Revised: February 26, 2012

Published: February 28, 2012

that helix 1 undergoes a helix–coil conformational change in solution.^{22,23}

The inherent conformational dynamics that regulate the partitioning of helix 1 in the FAT domain are thought to play a role in the phosphorylation of Y926 by Src and in the binding of the phosphorylated FAT domain to the Grb2 SH2 domain.^{19,21} Structural studies of kinases bound to substrate peptides suggest that the kinase recognizes an extended conformation for phosphorylation.²⁴ Furthermore, structural evidence also suggests that Y926 must exist in a β -turn conformation to bind to Grb2.^{25–28} However, because Y926 in the FAT domain is in a helix, it is not in a conformation that is conducive to phosphorylation by Src or binding to Grb2. Therefore, it has been suggested that there must be a conformational change near Y926 to facilitate phosphorylation by Src and binding to the Grb2 SH2 domain.^{19,21}

While it has been proposed that conformational dynamics in the FAT domain are important for regulating phosphorylation of Y926 and binding to Grb2, the mechanism(s) that regulates FAT domain dynamics in vivo is unclear. In this paper, we explore the effect of pH on the structure, dynamics, and Src-mediated phosphorylation of the FAT domain in vitro.

■ EXPERIMENTAL PROCEDURES

Expression and Purification of the FAT Domain. The FAT domain was expressed as a GST fusion protein and purified as previously described.¹⁹

Expression and Purification of the Src Kinase Domain. Plasmids containing the kinase domain of c-Src and the YopH phosphatase were provided by J. Kuriyan's lab at the University of California (Berkeley, CA). The expression and purification of the kinase domain of avian c-Src (251–533) have been described previously.²⁹ The purified protein was stored in 50% glycerol at -20°C until it was used.

In Vitro Src-Mediated Phosphorylation of the Full-Length FAT Domain. The purified FAT domain was dialyzed into phosphorylation buffer [100 mM MES (pH 5.5, 6.0, or 6.5) or 100 mM HEPES (pH 7.0 or 7.5), 5.0 mM MgCl_2 , 1 mM DTT, and 0.01% NaN_3]. Each reaction mixture contained $\sim 30\ \mu\text{M}$ FAT domain, $\sim 1\ \mu\text{M}$ Src, and 1 mM ATP. Reaction mixtures were incubated at 37°C overnight in an Eppendorf tube with a 2 kDa molecular mass cutoff bottom floating in 100 mL of phosphorylation buffer to ensure that the pH remained constant throughout the course of the reaction. Samples were dialyzed into water before MS analysis.

In Vitro Src-Mediated Phosphorylation of FAT Domain Synthetic Peptides. Two synthetic peptides containing either Y926 (SNDKV⁹²⁶YENVTLGLVK-OH) or Y1008 (MKLAQQ¹⁰⁰⁸YVMTSLQQEYK-OH) were synthesized at the University of North Carolina High-Throughput Peptide Synthesis and Arraying Facility. The peptides were dissolved in water and diluted with 10 \times phosphorylation buffer to a final concentration of 0.56 mg/mL in a final volume of 100 μL . Src (1 μL of a 5 mg/mL solution) was added to each reaction mixture, and the mixtures were incubated at 37°C for 1 h. In total, 10 reactions were performed: phosphorylation of the Y926 peptide and the Y1008 peptide, each at pH 5.5, 6.0, 6.5, 7.0, and 7.5. Samples were kept at -20°C until they were analyzed.

Mass Spectrometry-Based Phosphopeptide Identification. The sites of phosphorylation were identified by liquid chromatography–tandem mass spectrometry (LC–MS/MS) analysis of tryptic peptides derived from the phosphorylation

reaction between FAT and Src. The experimental workflow is shown in Figure S1 of the Supporting Information. The FAT domain was phosphorylated as described above, and the samples were digested with trypsin. The digestion reaction was monitored by sodium dodecyl sulfate–polyacrylamide gel electrophoresis to ensure that the reaction had reached completion. The digestion reaction mixtures were spiked with the phosphopeptide internal standards, resuspended in an aqueous solution of 0.1% formic acid, and analyzed by reverse-phase LC–MS/MS using a nano ultra LC system (Eksigent Inc., Dublin, CA) coupled to an LTQ–Orbitrap Velos system (Thermo Scientific, San Jose, CA). The LC–MS/MS data were analyzed as previously described.³⁰ In brief, mass spectrometric data were acquired using the data-dependent mode to interrogate the top 10 most abundant peptide ions via collision-activated dissociation (CAD)–MS/MS. Mass spectra were processed, and peptide identification was performed using Mascot (Matrix Science Inc.). Peptides were identified using a target decoy approach with a false discovery rate (FDR) of 1%. The Ascore algorithm was used to confidently localize the phosphorylation site on the peptide derived from the sample.³¹ In addition, the synthetic phosphopeptide standards were used to further verify the phospho-site assignment specificity using retention time and fragmentation patterns.

Peptide Quantitation. Absolute quantitation of site-specific phosphorylation was performed on the peptides that contained the two identified phosphorylation sites in the FAT domain (pY926 and pY1008) with spiked-in heavy labeled internal standards. The following four phosphopeptide internal standards containing a ^{13}C -labeled valine residue were synthesized at the University of North Carolina High-Throughput Peptide Synthesis and Arraying Facility: V(p⁹²⁶Y)-ENVTLGL(V¹³C5)K-OH, SNDKV(p⁹²⁶Y)ENVTLGL(V¹³C5)K-OH, LAQQ(p¹⁰⁰⁸Y)(V¹³C5)MTSLQQEYK-OH, and MKLAQQ(p¹⁰⁰⁸Y)(V¹³C5)MTSLQQEYK-OH. In addition to the tryptic peptides, we also introduced an additional peptide standard for each site to compensate for possible variations in digestion efficiencies that would yield phosphopeptides containing a missed cleavage site. The internal standards were spiked, separately, at three or four standard concentrations (0.2, 0.4, 1, and 2 $\mu\text{g/mL}$) into the FAT trypsin digestion reaction mixtures. The raw peaks were processed, and extracted ion chromatograms (XIC) were generated via full-scan MS using Xcalibur (Thermo Scientific). Peptide peaks of interest were normalized by their stable isotope-labeled heavy internal standard counterparts using an in-house Perl script. Peak integration was performed using the Genesis algorithm (Thermo-Fisher Scientific, San Jose, CA). All deviations in retention times were corrected by peak alignment. The accuracy of the peak area ratios was validated by acquiring multiple chromatographic runs as described previously.³⁰ Absolute quantitation was based on the relative peak area of the identified phosphopeptide and the corresponding heavy phosphopeptide internal standard. A standard curve was generated by plotting the log of the normalized peak area (area of analyte/area of standard) versus the standard concentration. The curves were fit by linear regression in Excel, and the x -intercept of the fit represents the analyte concentration. Both +3 and +2 charge states were quantified using these standard curves.

Relative changes in phosphorylation levels of the synthetic peptides were quantified as a function of pH using a single standard concentration (0.5 $\mu\text{g/mL}$ heavy internal standard).

Phosphorylation reaction mixtures with the peptide containing Y926 were diluted 100-fold before being analyzed by MS, whereas reaction mixtures of the peptide containing Y1008 were diluted 4-fold before being analyzed by MS so that the signal was in an appropriate linear dynamic range for quantitation.

Circular Dichroism. The purified FAT domain was dialyzed into CD buffer (10 mM K_2HPO_4 and 0.01% NaN_3) at the desired pH and concentrated to 10 μ M. Far-UV CD (185–260 nm) spectra were recorded at 25 °C on an Applied Photophysics Pistar-180 spectropolarimeter. Thermal denaturation studies were conducted by monitoring the ellipticity at 221 nm over a temperature range of 25–95 °C in increments of 0.5 °C. Far-UV CD spectra (from 185 to 260 nm) collected after the FAT domain had been heated to 95 °C for 30 min showed that the FAT domain retained little or no helical character at 95 °C. After each thermal denaturation, the temperature was reduced to 25 °C for 15 min, and a far-UV spectrum was collected to verify that the FAT domain had regained its secondary structure.

Data analysis was conducted with the assumption that only populations of folded (F) and unfolded (U) species were being monitored. The denaturation curves were baseline corrected and fit to the following Boltzmann equation in SigmaPlot:

$$\theta_{obs} = \frac{25^\circ C + (\theta_F - \theta_U)}{1 + e^{(T_m - temp)/slope}}$$

θ_{obs} , θ_F , and θ_U are the observed ellipticity at 221 nm, the ellipticity at 221 nm of the folded FAT domain, and the ellipticity at 221 nm of the unfolded FAT domain, respectively. T_m is the melting temperature or the temperature at which half of the FAT domain is folded. Although the high temperature(s) required for most of the thermal denaturation studies limited the accuracy by which θ_U could be measured, the data were also fit to alternate equations,^{32,33} and similar results were obtained.

NMR Spectroscopy. The ^{15}N -labeled FAT domain and the ^{15}N - and ^{13}C -labeled FAT domain were expressed and purified as previously described.¹⁹ The purified FAT domain was exchanged into NMR buffer at the desired pH (25 mM Tris maleate, 150 mM NaCl, 10% D_2O , and 0.01% NaN_3) and concentrated to ~0.2 mM. All NMR data were processed with NMRPipe³⁴ and analyzed with NMRView.³⁵

1H – ^{15}N HSQC spectra were collected as a function of pH, and a simultaneous three-dimensional (3D) ^{13}C – ^{15}N NOESY^{36,37} spectrum with a 150 ms mixing time was collected at pH 6.0 and 7.5 on a Varian INOVA 800 MHz spectrometer at 37 °C. While temperature changes in some buffered solutions can affect the pH, we used a Tris-maleate buffer, which is relatively insensitive to temperature changes. The spectra were referenced to each other using peaks associated with the glycine linker.

Backbone assignments for the FAT domain at pH 6.0 had been obtained previously.¹⁹ Because several backbone resonances undergo chemical shift changes between pH 6.0 and 7.5, 3D NMR HNCACB³⁸ and CBCACONH³⁷ experiments were conducted at pH 7.5 on a sample of uniformly ^{13}C - and ^{15}N -labeled FAT domain, and backbone assignments at pH 7.5 were determined as previously described¹⁹ using the assignments at pH 6.0 as a starting point. Assignments at intermediate pH values were determined by tracking changes in chemical shifts at pH 6.0 and 7.5.

Residual dipolar coupling (RDC) data were collected on a ^{15}N -labeled sample of the FAT domain (0.4 mM). Pf1 phage (7.5 mg/mL, ASLA Biotech Ltd.) was used as an alignment medium as previously described.¹⁹ 1H – ^{15}N HSQC-IPAP³⁹ spectra were collected in NMR buffer alone and in the presence of phage.

Backbone Relaxation Analysis. ^{15}N -based two-dimensional (2D) T_1 , T_2 , and heteronuclear NOE (HetNOE) spectra⁴⁰ were collected on uniformly ^{15}N -enriched FAT domain samples at pH 6.0 and 7.5 on a Varian INOVA 600 MHz spectrometer at 37 °C. Prior to data collection, the temperature was calibrated using a 100% MeOH standard sample. R_1 and R_2 relaxation rates were sampled with nine time points, three of which were collected in duplicate to estimate the error. Delay values of 48, 136, 250, 385, 540, 708, 892, 1000, and 1300 ms were used for T_1 and 7, 15, 23, 39, 62, 78, 93, 109, and 125 ms for T_2 experiments. Two experiments comprising the 1H – ^{15}N NOE were conducted in an interleaved fashion with a recycle delay ~5 s. The T_1 and T_2 data were analyzed by fitting the intensities of resolved amide peaks to a single-exponential decay, and the HetNOE data were analyzed by determining the difference in intensity between the irradiated and nonirradiated spectra using programs provided by the laboratory of A. Lee (University of North Carolina at Chapel Hill).

T_1 , T_2 , and HetNOE data were used to evaluate backbone motions on the picosecond to nanosecond time scale using the model-free formalism.⁴¹ The isotropic rotational correlation time (τ_m) was determined using the approach described by Dellwo and Wand.⁴² Rotational diffusion anisotropy was calculated using the local Di method⁴³ and the crystal structure of the FAT domain (Protein Data Bank entry 1K40). Backbone relaxation data were fit using an anisotropic correction ($D_{par}/D_{perp} = 2.22$ and 1.73 at pH 6.0 and 7.5, respectively) to minimize model selection error.⁴⁴ Backbone relaxation rates were fit to one- or two-parameter model-free models (S^2 , S^2 , and τ_e ; S^2 and R_{ex}) using a program, relxn2.2, provided by the laboratory of A. Lee.^{45,46}

RESULTS

Phosphorylation of the FAT Domain. Phosphorylation of Y926 has been implicated in the exclusion of FAK from focal adhesions and promotion of focal adhesion turnover,⁴⁷ cell adhesion, migration, invasion in vitro, and metastasis in vivo.¹⁶ Therefore, understanding how phosphorylation of Y926 affects FAK signaling on a structural level could provide key insights into how this site is involved in FAK-mediated cancer progression. We were interested in characterizing the phosphorylated species of the FAT domain because previous data from our lab and others have suggested that a structural rearrangement is necessary for recognition of the phosphorylated species by Grb2.^{19,21,23} The FAT domain was phosphorylated in vitro using the purified Src kinase domain. We varied several conditions, one of which was pH, to identify optimal conditions for phosphorylation. The site of phosphorylation was identified via microelectrospray Fourier transform ion cyclotron resonance mass spectrometry (μ FT-ICR). The full MS of the intact protein revealed that the FAT domain was phosphorylated at a single site. Top-down electron capture dissociation tandem mass spectrometry (ECD–MS/MS) of the phosphorylated peak revealed the presence of two sites of phosphorylation in the FAT domain, Y926 and Y1008, at all pH values (pH 5.5, 6.0, 6.5, 7.0, and 7.5) (data not shown).

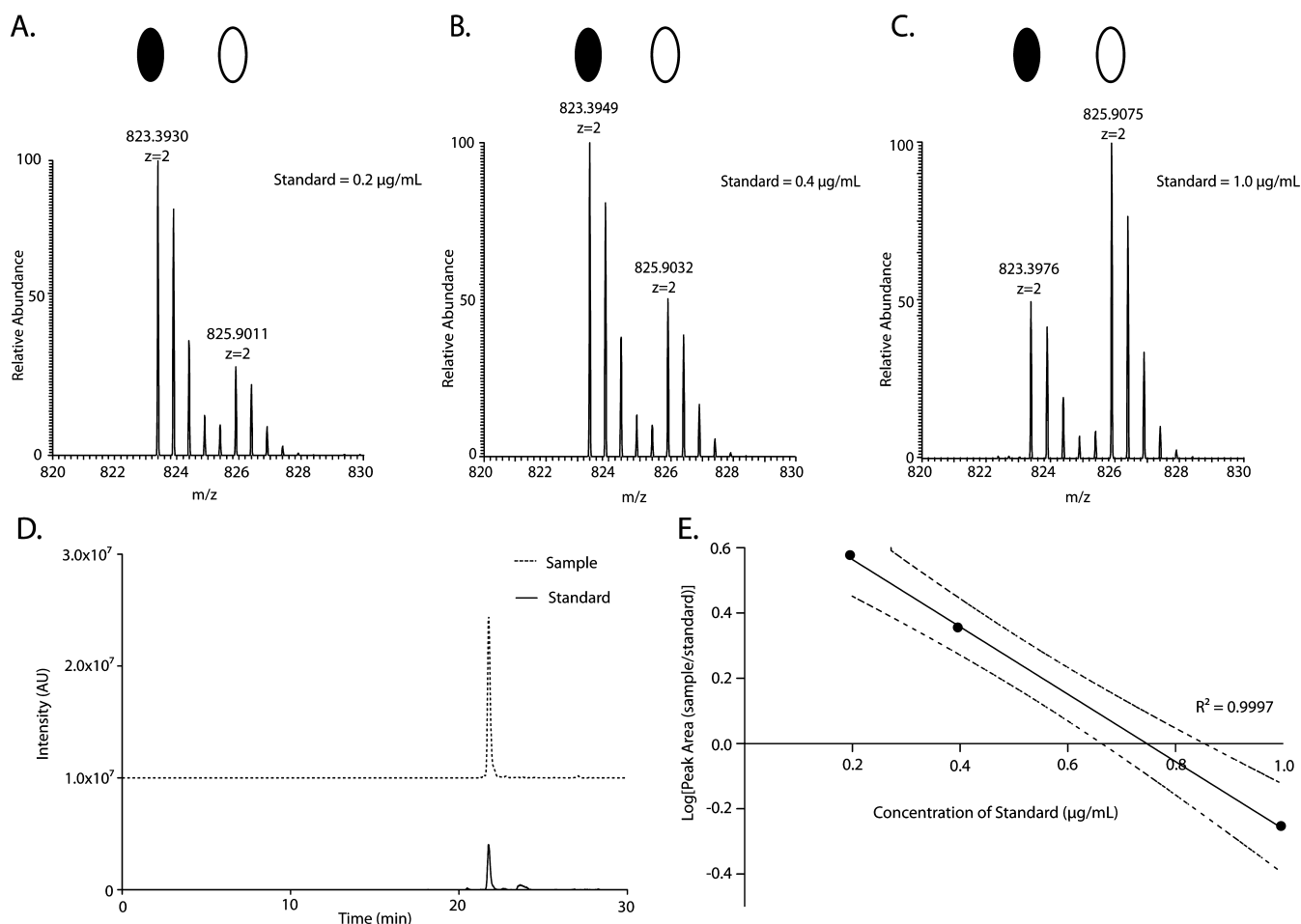


Figure 1. MS-based absolute quantification of the phosphopeptide containing Y926 ($z = +2$). MS spectra of the phosphopeptide containing Y926 with the corresponding sample peptide (filled oval) and heavy internal standard peptide (empty oval) spiked in at (A) 0.2, (B) 0.4, and (C) 1.0 $\mu\text{g/mL}$. (D) Extracted ion chromatogram (XIC) of the sample and internal standard spiked in at 0.2 $\mu\text{g/mL}$. (E) Linear regression fit of the normalized peak area of the sample as a function of spiked-in standard concentration. Dashed lines represent 95% confidence intervals.

Therefore, while we do not detect a doubly phosphorylated species, it appears that there are two sites of tyrosine phosphorylation in the FAT domain.

To verify the full-length phosphorylation site assignments and to quantify the relative phosphorylation levels of each site, we subjected the phosphorylated samples to trypsin digestion and analyzed the peptides by reverse-phase LC–MS/MS. Figures S2 and S3 of the Supporting Information show the unambiguous assignment of the two peptides phosphorylated at Y926 and Y1008 (>99% Mascot probability and Ascore corresponding to >99% site localization probability). The phosphorylation site assignments were further verified by their heavy labeled spiked-in internal standard peptide counterparts allowing concurrent verification of the sequence ions in the MS/MS spectra. It is noteworthy that the mass spectra are identical in terms of their fragmentation patterns and differ only when the product ions contain the heavy valine substitution.

The bottom-up CAD–MS/MS data show that the two phosphorylation sites in the FAT domain, Y926 and Y1008, were phosphorylated at a range of biologically relevant pH values (pH 5.5, 6.0, 6.5, 7.0, and 7.5) (data not shown), in agreement with the top-down ECD–MS/MS data. Y926 is the only site of tyrosine phosphorylation in the FAT domain reported to modulate FAK function. Whereas phosphorylation of Y1008 has been previously observed by mass spectrometry in

full-length FAK purified from Sf9 cells,⁴⁸ it was not identified as a Src substrate. Furthermore, it is unclear whether phosphorylation of Y1008 is physiologically relevant, and no prior studies have established the relative levels of phosphorylation between these distinct sites. To quantify the relative and absolute levels of phosphorylation at Y926 and Y1008, we used a stable isotope dilution mass spectrometry-based method. We spiked the trypsin digestion reactions with various concentrations of an internal standard, a synthetic ¹³C-labeled phosphorylated peptide with a sequence identical to that of the tryptic peptide. The spiked-in internal standard allows both absolute quantitation and sequence verification of the peptide of interest.

Figure 1 shows the stable isotope dilution mass spectrometry-based absolute quantification strategy that was used to determine the phosphorylation levels of Y926 at pH 5.5. The tryptic phosphopeptide that contains Y926 was quantified by the corresponding heavy-labeled spiked-in internal standard. The XIC peak areas of the phosphopeptide sample and internal standard (Figure 1D) were used to derive a linear relationship between the MS ion intensities and spiked-in standard. The linear regression of the standard curve, shown in Figure 1E, was then used to determine the absolute concentration of the phosphopeptide present in the sample at a given pH. We determined the concentration of both the +2 and +3 charge

states of each peptide phosphorylated at Y926 and Y1008 at pH 5.5, 6.0, 6.5, 7.0, and 7.5.

Figure 2A shows the levels of phosphorylation at Y926 and Y1008 as a function of pH. For Y926, phosphorylation levels

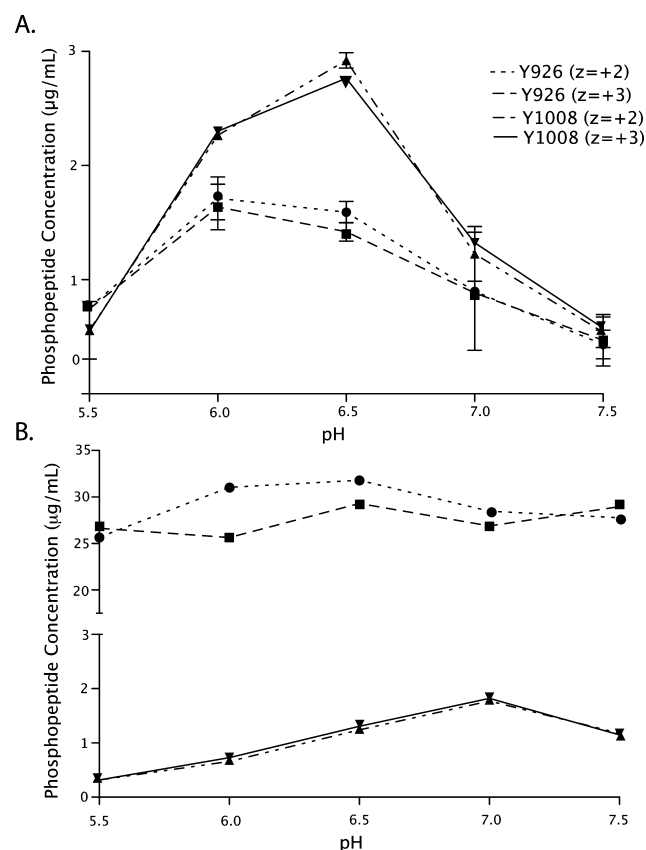


Figure 2. Site-specific quantitation of phosphorylation. (A) Full-length FAT domain and (B) FAT domain peptides were phosphorylated in vitro with Src kinase at pH 5.5, 6.0, 6.5, 7.0, and 7.5. After phosphorylation, the full-length FAT domain was trypsinized, and the levels of the Y926 phosphorylated peptide [(●) $z = +2$, and (■) $z = +3$] and Y1008 [(▲) $z = +2$, and (▼) $z = +3$] were quantified as described in the text. Comparison of the phosphorylation profiles of the full-length FAT domain and of FAT domain peptides reveals that the specificity of phosphorylation is different in the peptides and the full-length protein. Y1008 is preferred in the full-length FAT domain, whereas Y926 is preferred in the peptides. Furthermore, the pH dependence of phosphorylation of the peptides is different than that of the full-length protein.

are low at pH 5.5 ($0.75 \pm 0.04 \mu\text{g/mL}$), reach a maximum at pH 6.0 ($1.6 \pm 0.2 \mu\text{g/mL}$), and gently decrease to $0.4 \pm 0.2 \mu\text{g/mL}$ at pH 7.5. The pH profile for phosphorylation of Y1008 is slightly different. As seen for phosphorylation of Y926, phosphorylation levels of Y1008 are low at pH 5.5 ($0.5 \pm 0.2 \mu\text{g/mL}$) but reach a maximum at pH 6.5 ($2.85 \pm 0.06 \mu\text{g/mL}$) before sharply decreasing to $0.5 \pm 0.1 \mu\text{g/mL}$ at pH 7.5.

To determine whether the observed pH-dependent phosphorylation of the FAT domain is a result of the sensitivity of Src activity to pH or to pH-dependent changes in the FAT domain, we phosphorylated two synthetic peptides in vitro, one that contains Y926 and one that contains Y1008 (SNDKV⁹²⁶YENVNTGLVK-OH and MKLAQQ¹⁰⁰⁸-YVMTSLQQEYK-OH, respectively), at pH 5.5, 6.0, 6.5, 7.0, and 7.5 and subjected them to the same analysis as the full-

length protein. These peptides are expected to be unstructured, and therefore, their structure should not be influenced by pH. Figure 2B shows the pH profile for phosphorylation of the synthetic peptides. Phosphorylation of both peptides is relatively insensitive to pH. Therefore, we conclude that the pH-dependent phosphorylation observed in the full-length FAT domain is a result of a pH-dependent change in the conformation or dynamics of the FAT domain and not Src activity.

Interestingly, in the context of the peptide, Y926 is phosphorylated to a greater extent than Y1008 (~25-fold). This result differs from that of the full-length protein in which phosphorylation levels at the two sites were either comparable or Y1008 was the major site, depending on pH. The fact that the Y926 peptide is phosphorylated to a greater extent than the Y1008 peptide is consistent with the fact that Y926 is the biologically relevant site of phosphorylation and that, in the absence of structure, i.e., in the context of a peptide, the sequence surrounding Y926 is a better substrate for Src than the sequence surrounding Y1008. Consistent with this finding, the sequence surrounding Y926 (DKVYENVNT) is more similar to the Src consensus phosphorylation sequence (E/DEI/VYEGFF)⁴⁹ than that surrounding Y1008 (AQQYVMST).

pH-Dependent Thermal Unfolding of the FAT Domain. On the basis of the phosphorylation results, we believe that the pH-dependent phosphorylation observed in the full-length FAT domain is a result of a pH-dependent change in the conformation or dynamics of the FAT domain and not Src activity.

We therefore investigated the effects of pH on the secondary structure of the FAT domain by CD. Far-UV CD spectra collected at pH 5.5, 6.0, 6.5, 7.0, and 7.5 show no change in secondary structure (data not shown). Therefore, pH does not have a major effect on the helical content of the FAT domain.

We also investigated the pH dependence of the thermal stability of the FAT domain by CD. Figure 3 shows the thermal

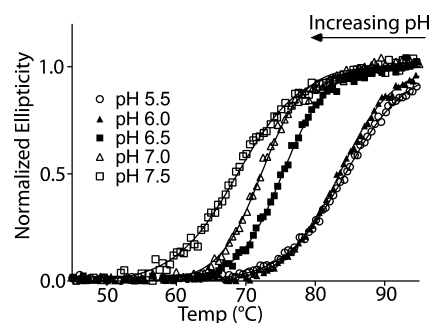


Figure 3. pH-dependent stability of the FAT domain. The thermal stability of the FAT domain was measured at pH 5.5, 6.0, 6.5, 7.0, and 7.5 by monitoring the CD signal at 221 nm from 25 to 95 °C. The FAT domain is significantly more stable at pH 5.5 than at pH 7.5, as indicated by the melting temperature.

denaturation curves at pH 5.5, 6.0, 6.5, 7.0, and 7.5. A sizable decrease in the T_m (approximately 16 °C) is observed as the pH is increased from 5.5 to 7.5. Because the CD data indicate that the FAT domain retains a helical content at higher pH values, the decrease in stability at higher pH values is likely a result of changes in tertiary packing interactions rather than the loss of secondary structure.

¹H-¹⁵N HSQC Spectrum of the FAT Domain as a Function of pH. To evaluate possible pH-dependent

perturbations on a per-residue basis, we collected high-resolution ^1H – ^{15}N HSQC spectra of the FAT domain at various pH values. The ^1H – ^{15}N HSQC spectrum provides the chemical shift for the amide nitrogen and proton atoms. The chemical shift value is sensitive to the electrochemical environment around that atom, and therefore, changes in chemical shift indicate that the environment around the atom

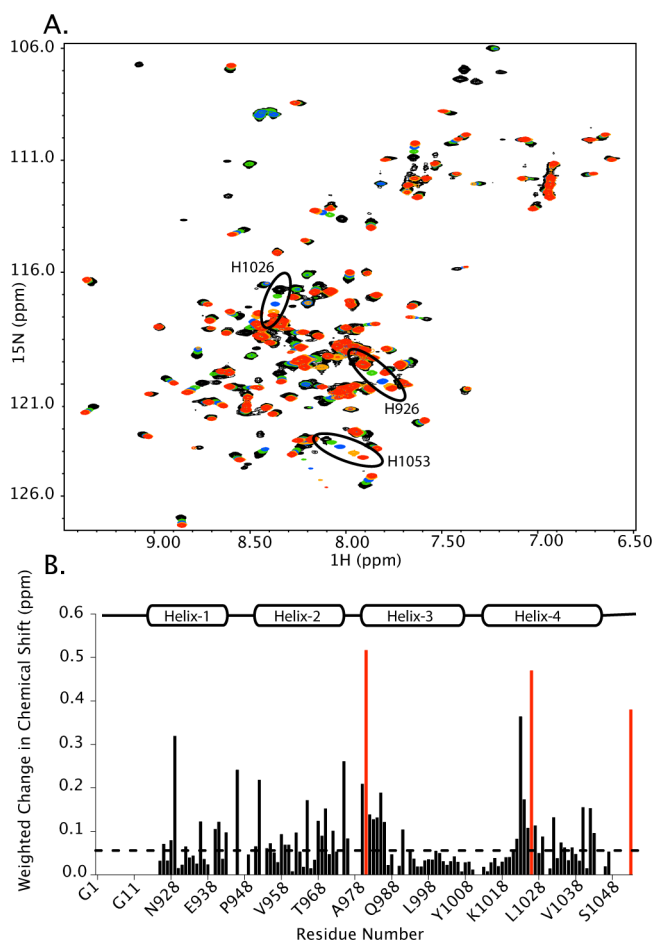


Figure 4. ^1H – ^{15}N HSQC spectra as a function of pH. (A) Overlay of ^1H – ^{15}N HSQC spectra collected at pH 5.5 (black), 6.0 (green), 6.5 (blue), 7.0 (orange), and 7.5 (red). The chemical shifts of several peaks are affected by pH, whereas others do not change. The chemical shifts of the three histidine residues in the FAT domain (H981, H1026, and H1053) are circled. (B) The weighted changes in chemical shift from pH 5.5 to 7.5 were calculated. Changes of >0.05 ppm (dashed line) were considered significant. Data for the histidine residues are colored red.

of interest is changing. Figure 4A shows an overlay of the ^1H – ^{15}N spectra at pH 5.5, 6.0, 6.5, 7.0, and 7.5. While some of the NH resonances show significant pH-dependent chemical shift changes ($\delta > 0.05$ ppm) over the pH range of 5.5–7.5, other NH resonances remain unchanged. Figure 4B shows the weighted changes in chemical shift mapped onto the sequence of the protein. Of interest is the fact that several residues with significant changes in chemical shift are in helix 1, which contains one of the sites of phosphorylation, Y926. In fact, one of the residues with the largest change in chemical shift is V929, which is near Y926. Furthermore, significant chemical shift changes are observed in the C-terminal end of helix 1 and in the

loop between helices 1 and 2. This region is of interest because dynamics in this region have been implicated in the regulation of Y926 phosphorylation.^{19,21} Our findings that NH resonances corresponding to residues near Y926 and regions thought to regulate phosphorylation of Y926 (the loop between helices 1 and 2) show pH-dependent changes in chemical shift support our MS results that demonstrate that Y926 phosphorylation is affected by pH.

The largest NH chemical shift changes were observed for the three histidine residues (H981, H1026, and H1053) in the FAT domain, which is not surprising because histidine side chains typically have pK_a values in the range of 6.0–6.5. We were able to track the chemical shift changes of the NH resonances of the histidine residues as a function of pH to estimate the pK_a of each histidine within the FAT domain. Figure S4 of the Supporting Information shows the titration profiles used to estimate pK_a values for each histidine. Estimated pK_a values for H981, H1026, and H1053 are 5.82 ± 0.04 , 6.21 ± 0.07 , and 6.5 ± 0.1 , respectively. Because these pK_a values are distinct, we proceeded to calculate the relative pK values of all the residues that showed significant chemical shift changes. Chemical shift changes that resulted in a pK value within ± 0.15 pH unit of one of the histidine pK_a values were considered correlated to that histidine. Figure S4d of the Supporting Information shows the residues whose pH-dependent changes in chemical shift correlate to specific histidine residues mapped onto the structure of the FAT domain. H981 and residues correlated to it are colored blue, whereas H1026 and correlated residues are colored red. Titration of H981, located at the beginning of helix 3, correlates with the pH-dependent NH chemical shift changes of nearby residues, as expected. However, there are also several residues distal to H981 whose pH-dependent NH resonances correlate with this residue, including residues all along helix 2 and in the amino terminus of helix 1, which contains Y926. Titration of H1026, located in the middle of helix 4, tracks with the pH-dependent NH chemical shift changes of surrounding residues. Interestingly, however, there are several residues in the C-terminus of helix 1 (V936, S940, S941, and S943) that titrate with H1026. Although the side chain of H1026 is mostly exposed to the solvent, the C-terminal region of helix 1 packs against helix 4 near H1026, and changes in helix 4 resulting from the titration of H1026 could affect residues in helix 1. These residues (V936, S940, S941, and S943) are near the loop between helices 1 and 2, which has been proposed to be involved in the regulation of Y926 phosphorylation.^{19,21} Histidine 1053, the last residue in FAK, does not appear to interact with other residues within the FAT domain, and titration of H1053 does not correlate with the pH-dependent changes in chemical shift of nearby residues. There were also a number of peaks, notably in the N-terminal region of helix 2, whose pH-dependent chemical shifts do not track with a particular histidine residue. pH-dependent NH chemical shift perturbations of these residues may be a result of protonation or deprotonation of both H1026 and H981 or of another titrating residue, possibly an aspartate or glutamate residue.

pH-Dependent Residual Dipolar Couplings. Because the ^1H – ^{15}N HSQC spectra (Figure 4) show significant changes in chemical shift as a function of pH, we collected NH RDCs at pH 6.0 and 7.5 to further investigate possible pH-dependent structural changes in the FAT domain. RDCs provide long-range orientation information about the NH bond vector and are often used to assess structural perturbations upon

mutation⁵⁰ and ligand binding.⁵¹ We chose pH 6.0 because the solution structure of the FAT domain had been determined at this pH.¹⁹ We were able to compare 47 of a possible 138 NH resonances (146 residues minus 8 prolines), using Pf1 phage to induce weak alignment of the sample. Figure S5 of the Supporting Information shows the correlation between RDC values of two data sets collected at pH 6.0, two data sets collected at pH 7.5, and a comparison of a data set collected at pH 6.0 and 7.5. The correlation between the RDC values at pH 6.0 and 7.5 was 0.85, which is not significantly different from the correlation between two data sets collected at pH 6.0 (0.88) or two data sets collected at pH 7.5 (0.90). Therefore, the RDC data do not indicate a major structural change in the FAT domain from pH 6.0 to 7.5.

NOE Analysis near Sites of Phosphorylation. To further assess possible structural alterations surrounding the two sites of phosphorylation as a function of pH, we collected a 3D ¹³C/¹⁵N NOESY spectrum at pH 6.0 and 7.5. Figure S6 of the Supporting Information shows the NOESY strips for H δ and H ϵ of Y926, while Figure S7 of the Supporting Information shows the NOESY strips for H δ and H ϵ of Y1008 at pH 6.0 and 7.5. While there are minor changes in NOE intensity, the number of NOEs at the two pH values is similar, suggesting that the side chains of both of these tyrosines maintain short-range (generally detected within 5 Å) NOE contacts as a function of pH. NOESY strips of other residues at the two pH values also show significant similarities.

¹H–¹⁵N HSQC Analyses Suggest pH-Dependent Changes in FAT Domain Dynamics. While we were unable to detect any significant pH-dependent structural change, there are several residues in the ¹H–¹⁵N HSQC spectra that show changes in NH peak intensity as a function of pH, suggesting a pH-dependent change in dynamics. In particular, as the pH is increased from 6.0 to 7.5, several residues show significant decreases in intensity resulting from peak broadening. Exchange broadening of NH resonances as the pH is increased can be difficult to interpret because a variety of mechanisms can contribute to this broadening, the most pertinent of which are pH-dependent differences in conformational dynamics (exchange between two or more states) and chemical exchange (an increase in the extent of exchange between the amide proton and the solvent). As expected, the N- and C-terminal NH resonances are severely broadened at higher pH, likely because of an increase in the level of base-catalyzed amide exchange. These residues are located in unstructured regions and consequently are more exposed to the solvent. There are also several NH resonances associated with residues in the turn between helices 3 and 4 and in the N-terminus of helix 4 that broaden as the pH is increased. Figure 5A shows the residues that broaden as the pH is increased mapped onto the structure of the FAT domain. Interestingly, these residues are located near Y1008, one of the sites of phosphorylation. However, as stated above, it is difficult to distinguish whether broadening in this region is due conformational or chemical exchange. However, an increase in the extent of solvent exchange is likely, as these residues are in a turn and exposed to the solvent.

In addition to peaks that broaden as the pH is increased, there are also several peaks that increase in intensity with an increase in pH from 6.0 to 7.5. Interestingly, several of these peaks are located at the end of helix 1, the beginning of helix 2, and the loop region between these helices. Figure 5B shows the peaks that increase in intensity as the pH is increased mapped onto the structure of the FAT domain. Several of these residues

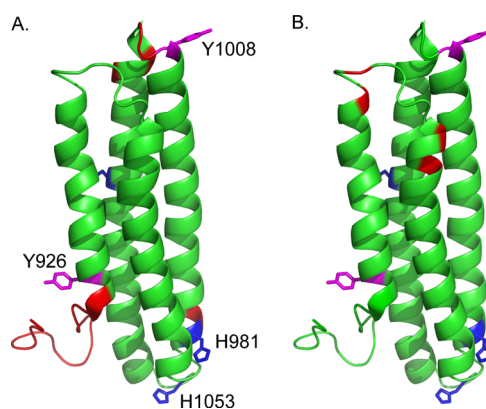


Figure 5. pH-dependent changes in intensity derived from ¹H–¹⁵N HSQC spectra. (A) Peaks that broaden in the ¹⁵N–¹H HSQC spectra from pH 5.5 to 7.5 are colored red. These residues localize to the N- and C-termini, the turn between helices 3 and 4, and the N-terminus of helix 4. (B) Peaks that narrow from pH 5.5 to 7.5 are colored red. These residues localize to the “hinge region” between helices 1 and 2. The two sites of phosphorylation, Y926 and Y1008, are colored magenta, and the histidine residues are colored blue.

were previously shown to be sensitive to temperature-dependent broadening,¹⁹ indicating that these residues experience dynamics on the intermediate to fast time scale. Conformational exchange in this region has previously been postulated to affect phosphorylation of Y926 in helix 1.^{19,21,22} While it is possible that this region is becoming less dynamic, the residues that narrow as the pH is increased are the same residues that narrow as the temperature is increased. Hence, it is likely that increasing the pH enhances the kinetics of the process that contributes to the exchange-mediated dynamics in this region, most likely reflecting a transition from the intermediate time scale, where peaks are broader, to a faster time scale, where peaks become sharper.

Backbone Dynamics. Because the pH-dependent ¹H–¹⁵N HSQC data suggest changes in dynamics as a function of pH, we further investigated this effect by collecting ¹⁵N backbone relaxation data (*T*₁, *T*₂, and HetNOE data sets) at pH 6.0 and 7.5. These measurements are sensitive to backbone dynamics on the picosecond to nanosecond time scale as well as the millisecond time scale. The relaxation data were fit to a model-free formalism^{41,42} to obtain the overall correlation time (τ_m) and order parameters *S*² and τ_e , which measure the rigidity of the N–H bond and the internal correlation time, respectively. Changes in pH over this range did not affect the overall correlation time (τ_m) of the protein, which is generally dependent on the overall size and shape of the molecule. The isotropic τ_m was determined to be 11.3 ns at pH 6.0 and 7.5. This value is slightly higher than expected for a protein this size (~9.5 ns) likely because the FAT domain is not spherical (60 Å × 20 Å × 20 Å²⁰). Therefore, model-free fitting was performed using an anisotropic correction. Figure 6A shows the *S*² values at pH 6.0 and 7.5 mapped onto the sequence of the FAT domain. No discernible difference was observed in the *S*² order parameter as a function of pH. As expected, the *S*² values are near 0.9 in the structured regions of the proteins and decrease to around 0.8 in the loops and turns. Residues in the N- and C-termini cannot be viewed by NMR at pH 7.5 and have lower *S*² values at pH 6.0 (~0–0.6), as these residues are less structured than those in the helix bundle, are more exposed to the solvent, and likely undergo enhanced solvent-mediated

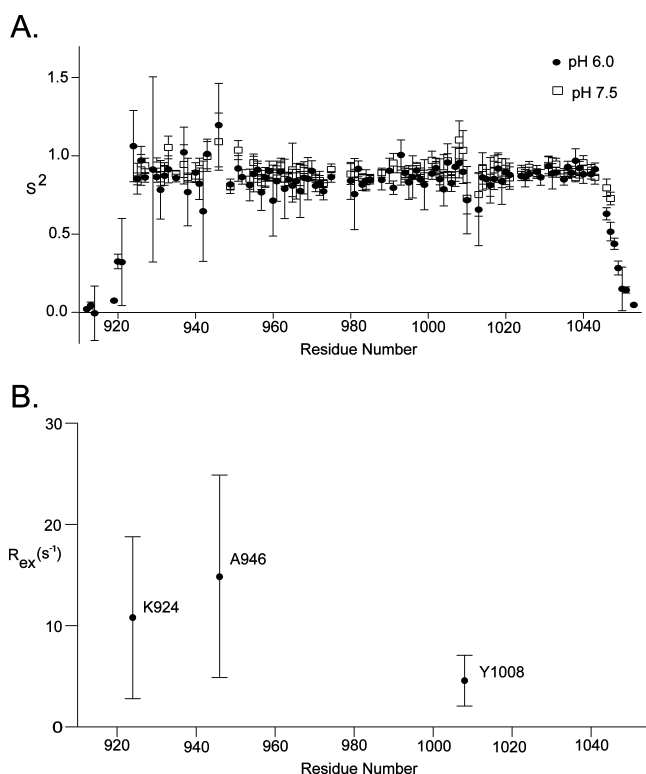


Figure 6. Backbone dynamics as a function of pH derived from 2D T_1 , T_2 , and HetNOE data as described in Experimental Procedures. (A) S^2 order parameters at pH 6.0 and 7.5 mapped onto the sequence of the FAT domain. (B) R_{ex} values at pH 6.0.

chemical exchange. Moreover, no difference in τ_c is observed as a function of pH.

It may not be surprising that we see little difference in S^2 or τ_c as a function of pH because these values are sensitive to backbone motions on faster time scales (picoseconds to nanoseconds) than the overall correlation time of the FAT domain. Thus, it is possible that the dynamic changes that occur as a function of pH occur on a slower time scale (microseconds to seconds) and may involve the side chains.

While the ^{15}N -based T_1 , T_2 , and NOE relaxation measurements provide dynamic information about the picosecond to nanosecond time scale, the measurements are also sensitive to motions on slower time scales (microseconds to milliseconds). Indeed, several residues appear to be undergoing motion on these slower time scales, as indicated by contributions from R_{ex} in the model-free fitting. At pH 6.0, there are three residues in helix 1, K924 (which is not visible at pH 7.5), A946, and Y1008, that experience slower microsecond to millisecond time scale dynamics (Figure 6B). The A946 NH resonance also narrows in the 1H - ^{15}N HSQC spectrum as the pH is increased, which provides further support that backbone dynamics in this region are susceptible to changes in pH. A946 is in a putative "hinge region", which consists of the loop between helices 1 and 2. It has been postulated that dynamics in this region due to strain caused by a series of proline residues modulate a helix-coil transition in helix 1 that regulates phosphorylation of Y926.¹⁹ It is also interesting that Y1008 displays pH-dependent microsecond to millisecond backbone dynamics as this is one of the sites of phosphorylation in the FAT domain, and our MS data indicate that phosphorylation at this site is sensitive to pH.

DISCUSSION

Phosphorylation of Y926 in the FAT domain has been shown to play a role in FAK signaling and localization. In particular, phosphorylation at this site has been linked to regulation of cell adhesion, migration, invasion in vitro, and metastasis in vivo.¹⁶ However, the mechanism by which phosphorylation of Y926 is regulated in vivo remains to be elucidated. While it has been suggested that a conformational change is necessary for phosphorylation of Y926,^{19,21} what regulates this change in vivo is unknown.

In this paper, we demonstrate that there are two sites of in vitro Src-mediated phosphorylation in the FAT domain: Y926 and Y1008. This is the first time to the best of our knowledge that Y1008 has been identified as a Src phosphorylation site. Furthermore, phosphorylation of these sites is pH-dependent. To distinguish whether the pH dependence of phosphorylation was due to pH-dependent changes in the FAT domain or in Src specificity, we phosphorylated two synthetic peptides corresponding to the tryptic fragments containing each of the FAT phosphorylation sites in vitro. Phosphorylation of the peptides does not show the same pH dependence as phosphorylation of the full-length FAT domain. We have interpreted the changes in phosphorylation of the peptides as being too minor to be significant. However, even if the changes in phosphorylation of the peptides are considered, they do not show the same trend as phosphorylation of the full-length FAT domain. We therefore conclude that the pH-dependent phosphorylation observed in the FAT domain is due to changes in the FAT domain and not Src. We have previously shown that phosphorylation of Y926 is sensitive to conformation. In the context of a GST-helix 1 construct, in which helix 1 is expected to be unstructured, Y926 is phosphorylated by Src to a greater extent than in the full-length FAT domain construct in vitro.¹⁹ Therefore, it is not surprising that we observe higher phosphorylation levels of the synthetic peptides than of the full-length FAT domain. However, it is interesting that the preference for Y926 or Y1008 is different in the peptides versus the full-length protein. In the context of the peptide, Y926 is phosphorylated to a greater extent than Y1008 (~25-fold), whereas in the full-length protein, the levels of phosphorylation are similar or Y1008 was the major site, depending on pH. While it is well-known that the proper sequence and conformation are necessary for recognition and subsequent phosphorylation by kinases, we think that this is an interesting example in which one site (Y926) appears to have a favorable sequence but a poor conformation for phosphorylation by Src whereas a second site (Y1008) has a poor sequence but a favorable conformation for phosphorylation. The fact that Y926 is the biological site of phosphorylation may suggest that, in vivo, sequence is more important than conformation for recognition by Src. However, the use of nonspecific phosphorylation antibodies and peptide libraries to investigate sites of phosphorylation and determine kinase consensus sequences may have resulted in Y1008 being overlooked as a possible substrate for Src. Further work is necessary to determine whether Y1008 is phosphorylated in vivo.

Regardless of the biological relevance of phosphorylation of Y1008, the phosphorylation data indicate that either the structure or dynamics of the FAT domain are sensitive to pH. NMR-derived backbone RDCs and NOEs collected at pH 6.0 and 7.5 do not support a pH-dependent structural change near

the two sites of phosphorylation. Furthermore, comparison of the solution structure determined at pH 6.0¹⁹ and the crystal structure determined at pH 7.0²¹ does not indicate a change in structure near Y926 or Y1008.

The second explanation for the observed pH-dependent phosphorylation is that a pH change over the range of 5.5–7.5 affects the conformational dynamics of the FAT domain. Amide resonances associated with the turn between helices 3 and 4 and the N-terminus of helix 4, which is near Y1008, show pH-dependent changes in intensity in the ¹H–¹⁵N HSQC spectrum, and the amide resonance of Y1008 shows microsecond to millisecond time scale motions. These data indicate that this region is in conformational exchange on this time scale and suggest that dynamics in this region may play a role in phosphorylation of Y1008.

A second region that experiences pH-dependent changes in dynamics is the loop between helices 1 and 2. Resonances in the ¹H–¹⁵N HSQC spectrum corresponding to this region narrow as the pH is increased, and we also observe microsecond to millisecond time scale motions in this region, suggesting that the loop between helices 1 and 2 is in exchange between two or more conformations on the microsecond to millisecond time scale. Indeed, previous NMR and hydrogen exchange-directed molecular dynamics data have suggested that dynamics in this region, due to strain caused by a series of proline residues, modulate a helix–coil transition in helix 1.^{19,22} An open, intermediate state of the FAT domain in which helix 1 is partitioned away from the bundle was detected.²² We have attempted to investigate backbone dynamics as a function of pH via CPMG-based relaxation dispersion experiments. However, we were unable to detect differences in *R*_{ex} with this experiment likely because the population of the open, intermediate state is too low to be detected by these measurements. Previous work with a Y926E mutant of the FAT domain demonstrated that the intermediate form is populated at 0.1%.²³ Hence, if a weakly populated pH-dependent state exists, it may be too weakly populated to be quantified by relaxation dispersion. Therefore, while we have evidence that dynamics in the hinge region and in the region near Y1008 are sensitive to pH on the microsecond to millisecond time scale, we were unable to quantify these dynamics.

Dynamics in the hinge region of the FAT domain have been proposed to control phosphorylation of Y926; however, what regulates these dynamics is unclear. On the basis of our data, it appears that pH affects dynamics in this region; however, we have not been able to quantify the rates and populations, possibly because of the presence of weakly populated states. Interestingly, the crystal structure of the domain-swapped dimer of the FAT domain was determined at pH 6.5, whereas the crystal structure of the monomeric four-helix bundle was determined at pH 7.0.²¹ It is unclear whether formation of the domain-swapped dimer was induced by the lower pH; however, it is possible that the lower pH favors partitioning of helix 1 and therefore the domain-swapped dimer. This is consistent with our observation that the level of phosphorylation of Y926 is higher at pH 6.5 than at pH 7.0, suggesting that a lower pH facilitates partitioning of helix 1, which would be expected to promote phosphorylation of Y926.

Because our results suggest that pH affects the dynamics of the FAT domain, we have attempted to determine the titrating residue that affects the dynamics. We have individually mutated the three histidine residues in the FAT domain as well as D994,

D1040, and E949 to alanine. The histidines were mutated because the NMR data indicate that the histidine side chains titrate over this pH range. The aspartate and glutamate mutants were chosen on the basis of their position in the structure of the FAT domain. D994 is in an area of negative charge, which might cause the side chain to be protonated; D1040 is in helix 4 and makes contacts with residues in helix 1 near Y926, and E949 is in the hinge region of the FAT domain. None of these mutants abrogate the pH-dependent stability of the FAT domain. It is possible that the pH-dependent effects that we observe are due to titration of a residue that we have not yet investigated or to titration of more than one residue.

This is the first study to quantitatively characterize the *in vitro* Src-mediated phosphorylation of the FAT domain of FAK. We have revealed that, *in vitro*, Src phosphorylates two tyrosine residues in the FAT domain, Y926 and Y1008. To the best of our knowledge, phosphorylation of Y1008 by Src has not been shown. We also show that phosphorylation of Y926 and Y1008 varies as a function of pH and that, although the pH profile of these two sites differs, we were unable to find conditions that would exclusively favor phosphorylation of one site over the other. Therefore, studies that involve phosphorylation of the FAT domain, particularly *in vitro*, should be carefully conducted to identify the site of phosphorylation. Furthermore, on the basis of our NMR, we believe that the pH dependence of phosphorylation of Y926 and Y1008 is due to changes in the dynamics of the FAT domain, which could represent an interesting means of regulating phosphorylation *in vivo*.

■ ASSOCIATED CONTENT

● Supporting Information

Determination of the sites of phosphorylation by mass spectrometry, including quantitation strategy and MS/MS spectra of phosphopeptides, titration profiles of histidine residues, pH-dependent RDC data, and pH-dependent NOE data for Y926 and Y1008. This material is available free of charge via the Internet at <http://pubs.acs.org>.

■ AUTHOR INFORMATION

Corresponding Author

*Telephone: (919) 966-7139. Fax: (919) 966-2852. E-mail: sharon_campbell@med.unc.edu.

Funding

This work was supported by National Institutes of Health Grant SR01GM080568-04 to S.L.C. and American Heart Association Predoctoral Grant 0815031E to J.C.

Notes

The authors declare no competing financial interest.

■ ACKNOWLEDGMENTS

We thank Dr. Greg Young and Dr. Ashutosh Tripathy for technical support in collecting the NMR and CD data, respectively. We also thank Dr. Mary Carroll in the laboratory of Dr. Drew Lee for help in analyzing the NMR relaxation data and Min-Qi Lu for extensive help in sample preparation.

■ ABBREVIATIONS

FAT, focal adhesion targeting; FAK, focal adhesion kinase; FERM, protein 4.1, ezrin, radixin, moesin; Grb2, growth factor receptor-bound protein 2; SH, Src homology; NHE1, sodium/proton exchanger 1; CAD, collision-activated dissociation;

FDR, false discovery rate; XIC, extracted ion chromatograms; RDC, residual dipolar coupling; HetNOE, heteronuclear nuclear Overhauser effect; μ FT-ICR, microelectrospray Fourier transform ion cyclotron resonance; ECD, electron capture dissociation.

REFERENCES

- (1) Schlaepfer, D. D., and Hunter, T. (1997) Focal Adhesion Kinase Overexpression Enhances Ras-dependent Integrin Signaling to ERK2/Mitogen-activated Protein Kinase through Interactions with and Activation of c-Src. *J. Biol. Chem.* 272, 13189–13195.
- (2) Ren, X., Kiosses, W., Sieg, D., Otey, C., Schlaepfer, D., and Schwartz, M. (2000) Focal adhesion kinase suppresses Rho activity to promote focal adhesion turnover. *J. Cell Sci.* 113, 3673–3678.
- (3) Hildebrand, J., Taylor, J., and Parsons, J. (1996) An SH3 domain-containing GTPase-activating protein for Rho and Cdc42 associates with focal adhesion kinase. *Mol. Cell. Biol.* 16, 3169–3178.
- (4) Tomar, A., Lim, S., Lim, Y., and Schlaepfer, D. (2009) A FAK-p120RasGAP-p190RhoGAP complex regulates polarity in migrating cells. *J. Cell Sci.* 122, 1852–1862.
- (5) Ilic, D., Furuta, Y., Kanazawa, S., Takeda, N., Sobue, K., Nakatsuji, N., Nomura, S., Fujimoto, J., Okada, M., Yamamoto, T., and Aizawa, S. (1995) Reduced cell motility and enhanced focal adhesion contact formation in cells from FAK-deficient mice. *Nature* 377, 539–544.
- (6) Webb, D. J., Donais, K., Whitmore, L. A., Thomas, S. M., Turner, C. E., Parsons, J. T., and Horwitz, A. F. (2004) FAK-Src signalling through paxillin, ERK and MLCK regulates adhesion disassembly. *Nat. Cell Biol.* 6, 154–161.
- (7) Zhao, J., Reiske, H., and Guan, J. (1998) Regulation of the cell cycle by focal adhesion kinase. *J. Cell Biol.* 143, 1997–2008.
- (8) Ryu, S. J., Cho, K. A., Oh, Y. S., and Park, S. C. (2006) Role of Src-specific phosphorylation site on focal adhesion kinase for senescence-associated apoptosis resistance. *Apoptosis* 11, 303–313.
- (9) Hungerford, J., Compton, M., Matter, M., Hoffstrom, B., and Otey, C. (1996) Inhibition of pp125FAK in cultured fibroblasts results in apoptosis. *J. Cell Biol.* 135, 1383–1390.
- (10) Schlaepfer, D. D., and Mitra, S. K. (2004) Multiple Connections link FAK to Cell Motility and Invasion. *Curr. Opin. Genet. Dev.* 14, 92–101.
- (11) Ilic, D., Almeida, E. A. C., Schlaepfer, D. D., Dazin, P., Aizawa, S., and Damsky, C. H. (1998) Extracellular Matrix Survival Signals Transduced by Focal Adhesion Kinase Suppresses p53-mediated Apoptosis. *J. Cell Biol.* 143, 547–560.
- (12) Xu, L., Owens, L., Sturge, G., Yang, X., Liu, E., Craven, R., and Cance, W. (1996) Attenuation of the expression of the focal adhesion kinase induces apoptosis in tumor cells. *Cell Growth Differ.* 7, 413–418.
- (13) Tachibana, K., Sato, T., D'Avirro, N., and Morimoto, C. (1995) Direct Association of pp125^{FAK} with Paxillin, the Focal Adhesion-Targeting Mechanism of pp125^{FAK}. *J. Exp. Med.* 182, 1089–1100.
- (14) Schlaepfer, D. D., and Hunter, T. (1996) Evidence for in vivo phosphorylation of the Grb2 SH2-domain binding site on focal adhesion kinase by Src-family protein-tyrosine kinases. *Mol. Cell. Biol.* 16, 5623–5633.
- (15) Katz, B.-Z., Romer, L., Miyamoto, S., Volberg, T., Matsumoto, K., Cukierman, E., Geiger, B., and Yamada, K. M. (2003) Targeting Membrane-localized Focal Adhesion Kinase to Focal Adhesions: Roles of Tyrosine Phosphorylation and Src Family Kinases. *J. Biol. Chem.* 278, 29115–29120.
- (16) Kaneda, T., Sonoda, Y., Ando, K., Suzuki, T., Sasaki, Y., Oshio, T., Tago, M., and Kasahara, T. (2008) Mutation of Y925F in focal adhesion kinase (FAK) suppresses melanoma cell proliferation and metastasis. *Cancer Lett.* 270, 354–361.
- (17) Mitra, S., Mikolon, D., Molina, J., Hsia, D., Hanson, D., Chi, A., Lin, S.-T., Bernard-Trifilo, J., Ilic, D., Stupack, D., Cheres, D., and Schlaepfer, D. (2006) Intrinsic FAK Activity and Y925 Phosphorylation Facilitate an Angiogenic Switch in Tumors. *Oncogene* 25, 1–16.
- (18) Ezratty, E., Partridge, M., and Gundersen, G. (2005) Microtubule-induced focal adhesion disassembly is mediated by dynamin and focal adhesion kinase. *Nat. Cell Biol.* 7, 581–590.
- (19) Prutzman, K. C., Gao, G., King, M. L., Iyer, V. V., Mueller, G. A., Schaller, M. D., and Campbell, S. L. (2004) The Focal Adhesion Targeting Domain of Focal Adhesion Kinase Contains a Hinge Region that Modulates Tyrosine 926 Phosphorylation. *Structure* 12, 881–891.
- (20) Hayashi, I., Vuori, K., and Liddington, R. C. (2002) The Focal Adhesion Targeting (FAT) Region of Focal Adhesion Kinase is a Four-Helix Bundle that Binds Paxillin. *Nat. Struct. Biol.* 9, 101–106.
- (21) Arold, S. T., and Hoellerer, M. K. (2002) The Structural Basis of Localization and Signaling by the Focal Adhesion Targeting Domain. *Structure* 10, 319–327.
- (22) Dixon, R. D. S., Chen, Y., Ding, F., Khare, S. D., Prutzman, K. C., Schaller, M. D., Campbell, S. L., and Dokholyan, N. V. (2004) New Insights into FAK Signaling and Localization Based on Detection of a FAT Domain Folding Intermediate. *Structure* 12, 2161–2171.
- (23) Zhou, Z., Feng, H., and Bai, Y. (2006) Detection of a Hidden Folding Intermediate in the Focal Adhesion Targetin Domain: Implications for its Function and Folding. *Proteins: Struct., Funct., Bioinf.* 65, 259–265.
- (24) Hubbard, S. R. (1997) Crystal Structure of the Activated Insulin Receptor Tyrosine Kinase in Complex with Peptide Substrate and ATP Analog. *EMBO J.* 16, 5573–5581.
- (25) Songyang, Z., Shoelson, S. E., McGlade, J., Olivier, P., Pawson, T., Bustelo, X. R., Barbacid, M., Sabe, H., Hanafusa, H., and Yi, T. (1994) Specific motifs recognized by the SH2 domains of Csk, 3BP2, fps/fes, GRB-2, HCP, SHC, Syk, and Vav. *Mol. Cell. Biol.* 14, 2777–2785.
- (26) Rahuel, J., Gay, B., Erdmann, D., Strauss, A., Garcia-Echeverria, C., Furet, P., Caravatti, G., Fretz, H., Schoepfer, J., and Grutter, M. G. (1996) Structural basis for specificity of GRB2-SH2 revealed by a novel ligand binding mode. *Nat. Struct. Mol. Biol.* 3, 586–589.
- (27) Ogura, K., Tsuchiya, S., Terasawa, H., Yuzawa, S., Hatanaka, H., Mandiyan, V., Schlessinger, J., and Inagaki, F. (1999) Solution Structure of the SH2 Domain of Grb2 Complexed with the Shc-derived Phosphotyrosine-containing Peptide. *J. Mol. Biol.* 289, 439–445.
- (28) Nioche, P., Liu, W.-Q., Broutin, I., Charbonnier, F., Latreille, M.-T., Vidal, M., Roques, B., Garbay, C., and Ducruix, A. (2002) Crystal structures of the SH2 domain of grb2: Highlight on the binding of a new high-affinity inhibitor. *J. Mol. Biol.* 315, 1167–1177.
- (29) Seeliger, M. A., Young, M., Henderson, M. N., Pellicena, P., King, D. S., Falick, A. M., and Kuriyan, J. (2006) High Yield Bacterial Expression of Active c-Abl and c-Src Tyrosine Kinases. *Protein Sci.* 14, 3135–3139.
- (30) Gunawardena, H., Huang, Y., Kenjale, R., Wang, H., Xie, L., and Chen, X. (2011) Unambiguous characterization of site-specific phosphorylation of leucine-rich repeat Fli-I-interacting protein 2 (LRRFIP2) in Toll-like receptor (TLR4)-mediated signaling. *J. Biol. Chem.* 286, 10897–10910.
- (31) Beausoleil, S., Villen, J., Gerber, S., Rush, J., and Gygi, S. (2006) A probability-based approach for high-throughput protein phosphorylation analysis and site localization. *Nat. Biotechnol.* 24, 1285–1292.
- (32) John, D. M., and Weeks, K. M. (2000) van't Hoff enthalpies without baselines. *Protein Sci.* 9, 1416–1419.
- (33) Allen, D. L., and Pielak, G. J. (1998) Baseline length and automated fitting of denaturation data. *Protein Sci.* 7, 1262–1263.
- (34) Delaglio, F., Grzesiek, S., Vuister, G. W., Zhu, G., Pfeifer, J., and Bax, A. (1995) NMRPipe: A multidimensional spectral processing system based on UNIX pipes. *J. Biomol. NMR* 6, 277–293.
- (35) Johnson, B. A. (2004) Using NMRView to visualize and analyze the NMR spectra of macromolecules. *Methods Mol. Biol.* 278, 313–352.
- (36) Pascal, S. M., Muhandiram, D. R., Yamazaki, T., Forman-Kay, J. D., and Kay, L. E. (1994) Simultaneous acquisition of ¹⁵N and ¹³C NOE spectra of proteins in H₂O. *J. Magn. Reson., Ser. B* 103, 197–201.

- (37) Grzesiek, S., and Bax, A. (1992) Correlating backbone amide and side chain resonances in larger proteins by multiple relayed triple resonance NMR. *J. Am. Chem. Soc.* 114, 6291–6293.
- (38) Wittekind, M., and Mueller, L. (1993) HNCACB, a high-sensitivity 3D NMR experiment to correlate amide-proton and nitrogen resonances with the α - and β -resonances in proteins. *J. Magn. Reson., Ser. B* 101, 201–205.
- (39) Ottiger, M., Delaglio, F., and Bax, A. (1998) Measurement of J and dipolar couplings from simplified two-dimensional NMR spectra. *J. Magn. Reson.* 131, 373–378.
- (40) Farrow, N. A., Muhandiram, R., Singer, A. U., Pascal, S. M., Kay, C. M., Gish, G., Shoelson, S. E., Pawson, T., Forman-Kay, J. D., and Kay, L. E. (1994) Backbone Dynamics of a Free and a Phosphopeptide-Complexed Src Homology 2 Domain Studied by ^{15}N NMR Relaxation. *Biochemistry* 33, 5984–6003.
- (41) Lipari, G., and Szabo, A. (1982) Model-free approach to the interpretation of nuclear magnetic resonance relaxation in macromolecules. 2. Analysis of experimental results. *J. Am. Chem. Soc.* 104, 4559.
- (42) Dellwo, M. J., and Wand, A. J. (1989) Model-independent and model-dependent analysis of the global and internal dynamics of cyclosporin A. *J. Am. Chem. Soc.* 111, 4571–4578.
- (43) Lee, L., Rance, M., Chazin, W., and Palmer, A. (1997) Rotational diffusion anisotropy of proteins from simultaneous analysis of ^{15}N and ^{13}C α nuclear spin relaxation. *J. Biomol. NMR* 9, 287–298.
- (44) Osborne, M., and Wright, P. (2001) Anisotropic rotational diffusion in model-free analysis for a ternary DHFR complex. *J. Biomol. NMR* 19, 209–230.
- (45) Clarkson, M. W., Gilmore, S. A., Edgell, M. H., and Lee, A. L. (2006) Dynamic coupling and allosteric behavior in a nonallosteric protein. *Biochemistry* 45, 7693–7699.
- (46) Lee, A. L., Flynn, P. F., and Wand, A. J. (1999) Comparison of H-2 and C-13 NMR relaxation techniques for the study of protein methyl group dynamics in solution. *J. Am. Chem. Soc.* 121, 2891–2902.
- (47) Katz, B. Z., Romer, L., Miyamoto, S., Volberg, T., Matsumoto, K., Cukierman, E., Geiger, B., and Yamada, K. M. (2003) Targeting membrane-localized focal adhesion kinase to focal adhesions: Roles of tyrosine phosphorylation and SRC family kinases. *J. Biol. Chem.* 278, 29115–29120.
- (48) Ciccimaro, E., Hevko, J., and Blair, I. A. (2006) Analysis of phosphorylation sites on focal adhesion kinase using nanospray liquid chromatography/multiple reaction monitoring mass spectrometry. *Rapid Commun. Mass Spectrom.* 20, 3681–3692.
- (49) Songyang, Z., Carraway, K. L., Eck, M. J., Harrison, S. C., Feldman, R. A., Mohammadi, M., Schlessinger, J., Hubbard, S. R., Smith, D. P., Eng, C., Lorenzo, M. J., Ponder, B. A. J., Mayer, B. J., and Cantley, L. C. (1995) Catalytic specificity of protein-tyrosine kinases is critical for selective signalling. *Nature* 373, 536–539.
- (50) Mauldin, R. V., and Lee, A. L. (2010) Nuclear magnetic resonance study of the role of M42 in the solution dynamics of *Escherichia coli* dihydrofolate reductase. *Biochemistry* 49, 1606–1615.
- (51) Amero, C. D., Byerly, D. W., McElroy, C. A., Simmons, A., and Foster, M. P. (2009) Ligand-Induced Changes in the Structure and Dynamics of *Escherichia coli* Peptide Deformylase. *Biochemistry* 48, 7595–7607.